FINAL YEAR PROJECT REPORT

# PERFORMANCE ANALYSIS OF SR-30 ENGINE USING JET TEST STAND


By

**AFAQ AHMED KHAN**

**PAK/20095025, 95 (A) EC**




ADVISOR

**DR ZAHID**

CO-ADVISOR

**DR TARIQ AMIN**



**COLLEGE OF AERONAUTICAL ENGINEERING**

**PAF ACADEMY ASGHAR KHAN, RISALPUR**

(FEBRURY 2024)

# PERFORMANCE ANALYSIS OF SR-30 ENGINE USING JET TEST STAND

By

**AFAQ AHMED KHAN**

**PAK/20095025, 95 (A) EC**


ADVISOR

**DR ZAHID**

CO-ADVISOR

**DR TARIQ AMIN**

Report submitted in partial fulfillment of the requirements for the degree of Bachelors of Engineering in Aerospace (BE Aerospace)

In

**COLLEGE OF AERONAUTICAL ENGINEERING**

**PAF ACADEMY ASGHAR KHAN, RISALPUR**

(FEBRURY 2024)

# Approval

It is certified that the contents and form of the project entitled "**PERFORMANCE ANALYSIS OF SR-30 ENGINE USING JET TEST STAND**" submitted by **AFAQ AHMED KHAN** have been found satisfactory for the requirement of the degree.

Advisor: **Dr Zahid**

Signature: _____
Date: _____

Co-advisor : **Dr Tariq Amin**

Signature: _____
Date: _____

# Dedication

Dedicated to **Allah Almighty**, the source of all wisdom and guidance, whose blessings and mercy have illuminated every step of my journey. To my dear **Parents**, your boundless love, unwavering support, and endless prayers have been my greatest strength and motivation. I am forever grateful for your nurturing presence in my life, and for Allah's divine guidance that has led me to this moment of achievement.

# Acknowledgment

Glory to the **Allah Almighty**, the Creator and Sustainer of the Universe, whose divine guidance has illuminated every step of my journey. From the beginning, His blessings have paved the way for my success, and I am profoundly grateful for His unwavering support.

I extend my heartfelt gratitude to those who have accompanied me through the challenges and triumphs of this journey. Firstly, to my esteemed research advisor, **Dr Zahid**, whose exceptional guidance and unwavering support have been instrumental in shaping my research work. I also express my sincere appreciation to my co advisor, **Dr Tariq Amin**, for their valuable insights and time dedicated to refining my work.

**To my beloved parents**, whose unconditional love and unwavering support have been my anchor throughout this journey, I owe an immeasurable debt of gratitude. Your sacrifices and encouragement have been the driving force behind my achievements, and I am profoundly grateful for everything you have done to help me reach this milestone. This journey would not have been possible without your unwavering belief in me.

In conclusion, I am deeply grateful to Allah Almighty, my research supervisor, committee members, and my parents for their invaluable contributions and unwavering support. Their guidance and encouragement have been essential to my academic and personal growth, and I am forever indebted to them for their role in my success.

# Abstract

The experiment measured various parameters for a gas turbine at intervals of 5000 RPM's from a minimum of 60000RPM to a maximum of 80000RPM. In this experiment, the main objective is to analysis the performance and efficiencies of the cycle as well as certain components within the gas turbine using the cold-air and air standard analysis. A relationship between thrust generation, fuel flow with respect to engine speed was shown that as the fuel flow increased the thrust generation increased. Also, it was seen that at all speeds the calculated thrust is always more than the actual, this demonstrates that the general peration of a gas turbine can never met anticipated performance values due to losses and irreversibilities. The equipment used was the S-R 30 turbojet engine and varies thermocouples and pressure sensors to measure temperature and pressure. These were then linked to a portable computer equipped with data acquisition software which recorded various parameters at 3 second intervals. The pressure ratio across the compressor increased to a maximum of 3. This led to efficiencies between 30% - 51% for the compressor. The compressor efficiency is also completely dependent on its pressure ratio. The turbine efficiency and other performance parameters for the turbine were inconclusive as there was a fuel delivery issue which lead to incomplete combustion. The SFC (Specific fuel consumption) expressions the fuel efficiency of the engine and was found to decrease with an increase in RPM. The lowest SFC was 0.000091 $\mathrm{m}^3/\mathrm{s}$ kN which occurred at 82982 RPM. As the test rig is stationary, the propulsion efficiency was calculated to be zero. Therefore, the thermal efficiency was used as a comparison to the Carnot efficiency. The thermal efficiency reached a maximum of 30% at the maximum RPM value of 82982 where the Carnot efficiency was 37%.

# Table of Contents

# List of Figures

# List of Tables

# Nomenclature

| Symbol | Description | Units |
|---|---|---|
| $\mathrm{P}_1$ | Compressor Inlet Pressure | Pa |
| $\mathrm{P}_2$ | Compressor Exit Pressure | Pa |
| $\mathrm{P}_3$ | Turbine Inlet Pressure | Pa |
| $\mathrm{P}_4$ | Turbine Exit Pressure | Pa |
| $\mathrm{P}_5$ | Nozzle Exit Pressure | Pa |
| $\mathrm{P}_{\mathrm{atm}}$ | Atmospheric Pressure | Pa |
| $\mathrm{T}_1$ | Compressor Inlet Temperature | K |
| $\mathrm{T}_2$ | Compressor Exit Temperature | K |
| $\mathrm{T}_{2\mathrm{s}}$ | Isentropic Compressor Exit Temperature | K |
| $\mathrm{T}_3$ | Turbine Inlet Temperature | K |
| $\mathrm{T}_4$ | Turbine Exit Temperature | K |
| $\mathrm{T}_{4\mathrm{s}}$ | Isentropic Turbine Exit Temperature | K |
| $\mathrm{T}_5$ | Nozzle Exit Pressure | K |
| $C_p$ | Specific Heat | KJ/kg |
| $C_v$ | Specific Heat | KJ/kg |
| $k$ | Specific Heat Ratio | Dimensionles |
| $\dot{m}_T$ | Total Mass Flow Rate | kg/s |
| $\dot{m}_{Air}$ | Mass Flow Rate of Air | kg/s |
| $\dot{m}_{Fuel}$ | Mass Flow Rate of Fuel | kg/s |
| SFC | Specific Fuel Consumption | kg/kg/s |
| E.G.T | Exhaust Gas Temperature | K |
| Thrust | Engine Thrust | kg |
| $V_1$ | Compressor Inlet Velocity | m/s |
| $V_5$ | Second Nozzle Exit Velocity | m/s |
| $ke_5$ | Second Nozzle Exit Kinetic Energy | kJ/kg |
| $\eta_c$ | Compressor Efficiency | % |
| $\eta_T$ | Turbine Efficiency | % |
| $\eta_b$ | Thermal Efficiency | % |

# Chapter 1

# INTRODUCTION

## 1.1 Project Title

## 1.2 Project Description

In an open gas turbine cycle as shown in Figure 1.1. Atmospheric air is continuously drawn into the diffuser to slow down the fast-moving air which is then compressed and ignited to causing the cycle to eventually become self-sustaining while still producing thrust out through the end nozzle which uses a reducing area to increase the exit fluid velocity which creates propulsion. Figure 1.2 represents a temperature entropy diagram for a turbojet engine [2].

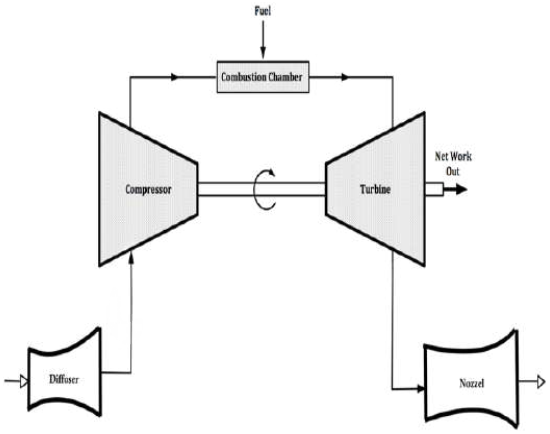


Figure 1.1: Schematic of Turbojet engine

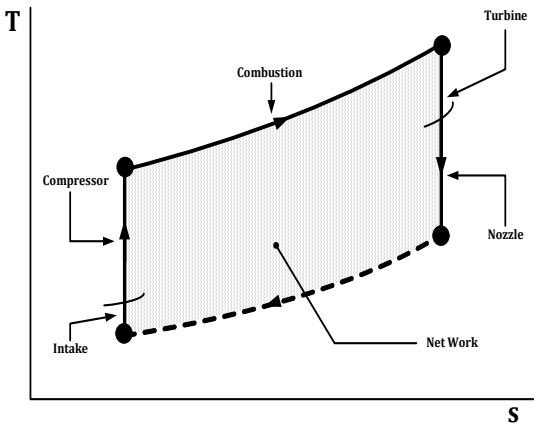


Figure 1.2: Ts diagram for a turbojet engine

### 1.2.1 Ideal Air Standard Analysis of the Brayton Cycle

The working fluid through the cycle is air, which behaves as an ideal gas. The temperature rise in the heat exchanger is due to heat transfer from an external source. With

this analysis, the complex combustion process and the change is the working fluid during the mixture is avoided. As a result, this modelling is a simple yet effective analysis of the gas turbine. If the Brayton cycle is further analysed on a cold-air standard, the variation in specific heats can be neglected. Figure 1.4 is a temperature entropy diagram illustrating the direction of energy transfer between the numbered points in the cycle

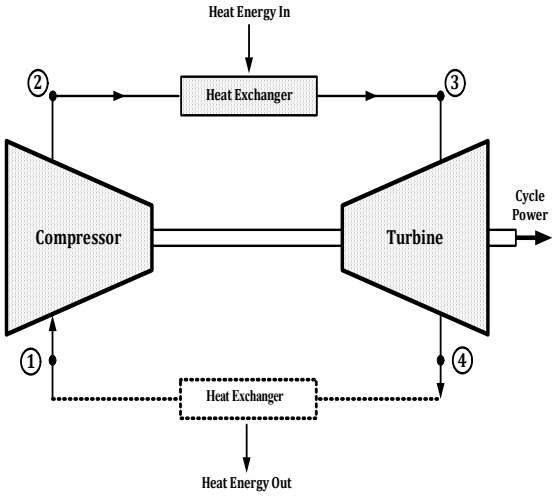


Figure 1.3: Air standard gas turbine cycle

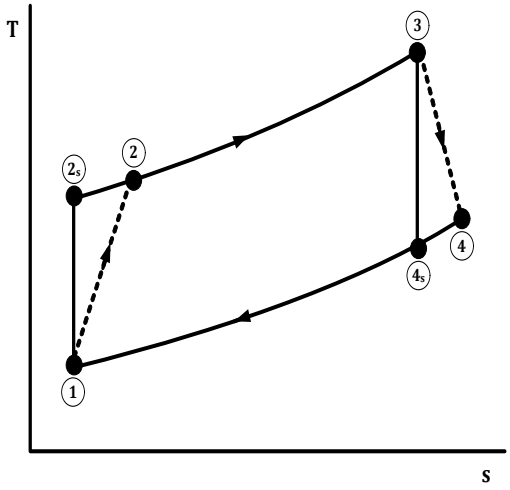


Figure 1.4: Ts diagram with irreversibilities

Using Figure 1.6 and the cold-air analysis the compressor exit temperature $T_{2s}$ can be calculated using Equation 1.1 with k being the specific heat ratio [5].

$$T_{2s} = T_1 \left( \frac{p_2}{p_1} \right)^{\frac{k-1}{k}} \tag{1.1}$$

Similarly, the turbine exit temperature $T_{4s}$ can be calculated using the respective values for the turbine [5]. Also from Figure 1.6, the compressor and turbine efficiencies can be deduced as stated in Equation 1.2 and 1.3 respectively.

$$\eta_C = \frac{T_1 - T_{2s}}{T_1 - T_2} \tag{1.2}$$

$$\eta_T = \frac{T_3 - T_4}{T_3 - T_{4s}} \tag{1.3}$$

Equation 1.1 to 1.3 can be applied using the air standard analysis by using the enthalpy values in place of the temperature values at each specific state. The thermal Carnot efficiency of the cycle is then represented by Equation 1.4 [1] which can also be represented as Equation 1.5:

$$\eta_b = 1 - \frac{T_1}{T_2} \tag{1.4}$$

$$\eta_b = 1 - \frac{1}{(P_2/P_1)^{\frac{k-1}{k}}} \tag{1.5}$$

The standard Brayton cycle [6] can be modified in different ways to benefit a specific end result. By manipulating the operating temperatures and pressure ratios, the thermal efficiency and net work of a cycle can be altered using Equation 1.2 to 1.5. This can be made clear in Figure 3.1 and 3.2 which illustrate how efficiency and work changes based on specific parameters.

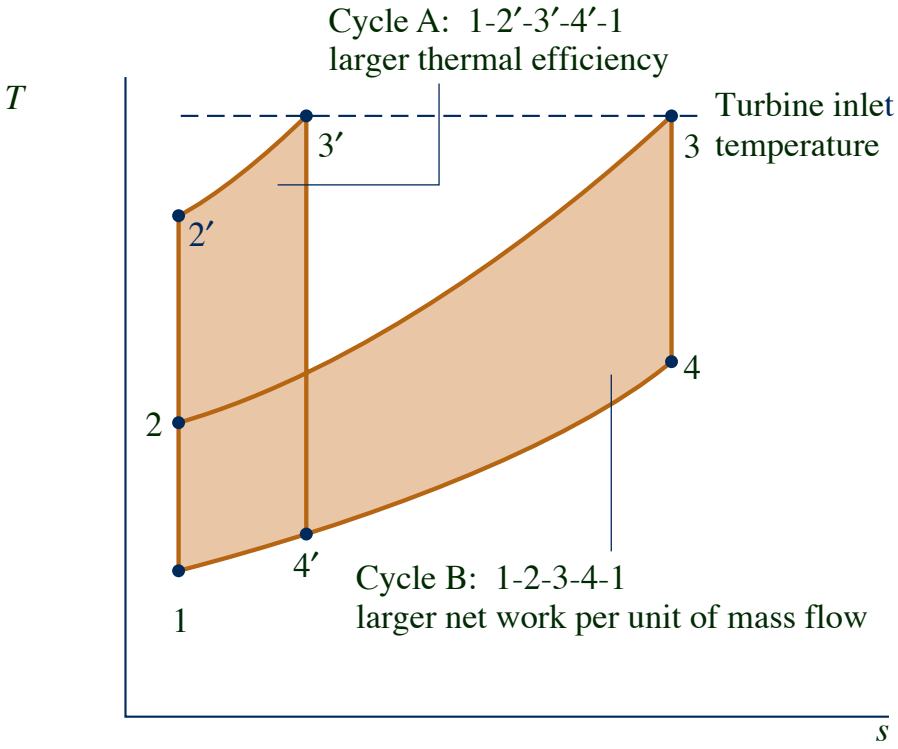


Figure 1.5: Ts diagram of two cycles with different parameters [1]

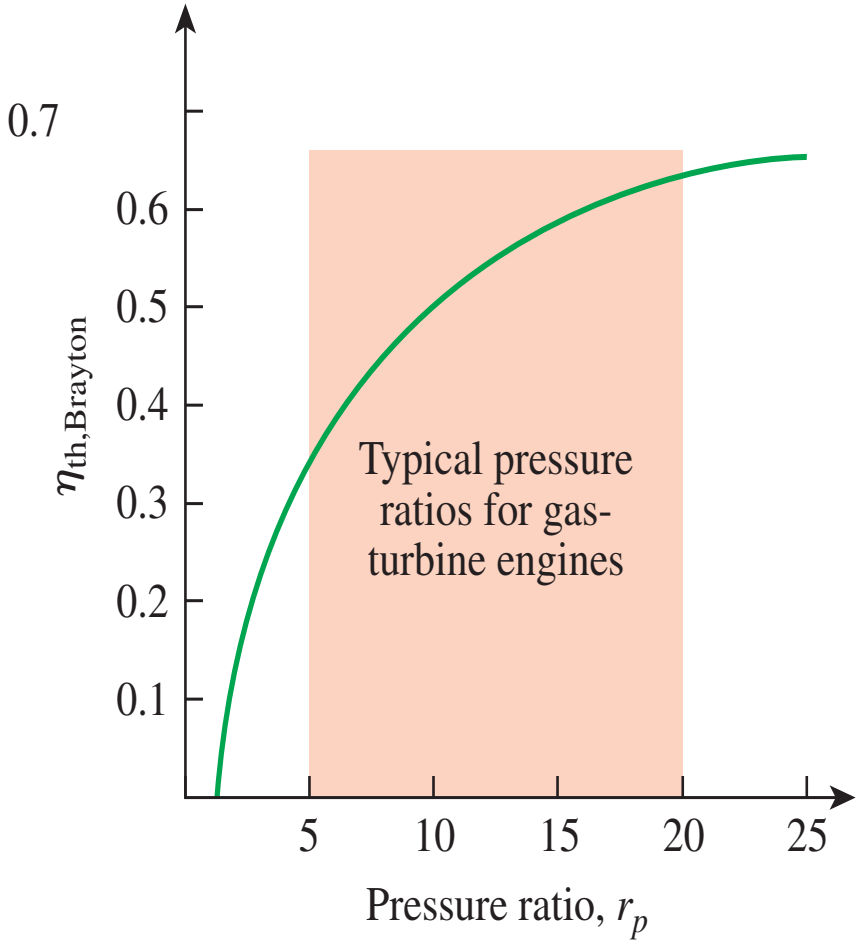


Figure 1.6: Thermal efficiency vs Compressor Pressure ratio [2]

### 1.2.2 Specific Fuel Consumption

This is the amount of fuel consumed by the jet engine per unit time per unit thrust [7]. It is an essential parameter to assess the performance of the different engines as it depicts the amount of fuel used [8]. The specific fuel consumption can be calculated using Equation 1.6:

$$SFC = \frac{\dot{m}}{Thrust} \tag{1.6}$$

where:

$$Thurst = \dot{m} * \textit{Exit Velocity} \tag{1.7}$$

### 1.2.3 Gas Turbines for Aircraft Propulsion

Turbojet engines are commonly used in aircrafts because they have a power to weight ratio of 6-10 kW/kg [9] which will increase efficiency as this helps minimising fuel consumption. The thermal efficiency formula for a jet engine is described in Equation 1.8, while the propulsion efficiency is described in equation Equation 1.9:

$$\eta_b = \frac{\dot{m}_{\text{air}}\ ke_5}{\dot{m}_{\text{fuel}}(\text{Calorific value})} \tag{1.8}$$

$$\eta_{propulsion} = \frac{2V_a}{V_s + V_a} \tag{1.9}$$

The work for the compressor and turbine can be analysed by conducting an energy balance across each component. The work for the turbine and compressor is calculated from Equation 1.10 and 1.11 respectively:

$$\dot{W}_t = \dot{m}(h_3 - h_4) \tag{1.10}$$

$$\dot{W}_c = \dot{m}(h_2 - h_1) \tag{1.11}$$

## 1.3 Motivation

The gas turbine is the primary method of propulsion for most modern aircrafts. The performance and efficiency of the engine directly associated with marking air travel more viable and increasing the commercial uses while decreasing the cost of fuel and lowering the amount of harmful gases in the atmosphere. If any advancements are made in the improvement of gas turbines, it would transform the aerospace industry to a new level with greater possibilities. By looking at each component it is necessary to analysis how different performance parameters, such as specific fuel consumption and efficiencies influence the system as a whole. This experiment investigates the performance of gas turbine in laboratory conditions and allows one to familiarise oneself with the components and operation.

## 1.4 Project Scope

- Analyse the performance of the turbine, compressor and the cycle in respect to engine speed.
- Calculate the efficiency of the turbine, compressor and the cycle efficiency with respect to the engine speed.
- Compare calculated efficiencies from measured data with expected theoretical efficiencies and the Carnot efficiency.
- Compare measured thrust generation with calculated theoretical thrust at different speeds.
- Determine a relationship between the specific fuel consumption of the engine with the variation of engine speed.
- Examine possible factors that dampen performance with viable reasons and provide possible solutions for better efficiencies.
- Compare the performance of the gas turbine during a hot run (increasing speed with fuel injection) verses a cold run (decreasing speed from a maximum speed).

## 1.5 Project Overview

The rest of the thesis is arranged in this way:

**Chapter 2**, Literature Review of the work done in this project.

**Chapter 3**, will discuss about the Experimental details and Methodology

**Chapter 4**, Results and performance will be discussed.

**Chapter 5**, result discussion and

**Chapter 6** presents the conclusions and recommendations regarding the project.

# Chapter 2

# LITERATURE REVIEW

## 2.1 Background and Overview

Turbines were first successfully built around the 1930's. The turbines built in this era had simple cycle efficiencies of approximately 17% [10] mainly because of low turbine and compressor efficiencies and low turbine inlet temperatures due to metallurgical limitations [11]. Steam turbines were then developed and initially used in power plants for power generation as turbines became capable of producing large amounts of power in the excess of 500 MW with efficiencies of close to 35% [11]. However, the steam turbines large furnaces made it impossible to incorporate into mobile applications. This lead to the development of gas turbines. Gas turbines rotate directly in the hot combustion gases therefore allowing the design to become more compact. With this new design, the gas turbines could now be used for aircraft propulsion.

## 2.2 Components of a Gas Turbine

The fundamental working principle of a gas turbine is to suck air in through the compressor which will increase the pressure of the air before passing it into the heat exchanger. In the heat exchanger fuel is added at high temperatures to the high-pressure air where it self-ignites. The process further increases the temperature of the air while creating an air-fuel mixture. This mixture then passes through the turbine which primary function is to drive the compressor. The residual mixture is channelled through the exhaust. The exhaust uses a variable area nozzle that can vary the velocity of the fluid which thereby changes the amount of thrust produced [12].

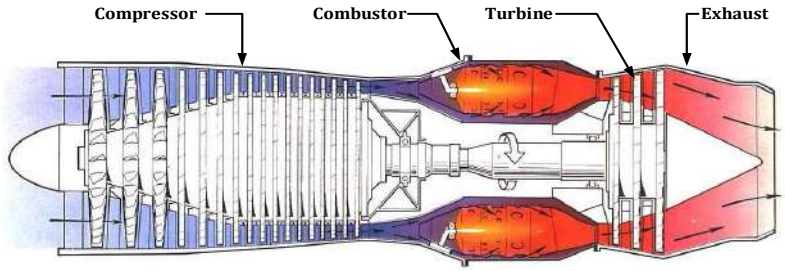


Figure 2.1: Major components in a Jet engine [3]

## 2.3 The Compressor

Gas turbine efficiencies are largely dependent of the pressures that can to generated by the compressor. Because of this, high performance engines incorporate multi-stage compressors which allows a greater pressure ratio to be achieved as well as better performance. Figure 2.2 is an illustration of a triple spool compressor which is used in high performance jet engines.

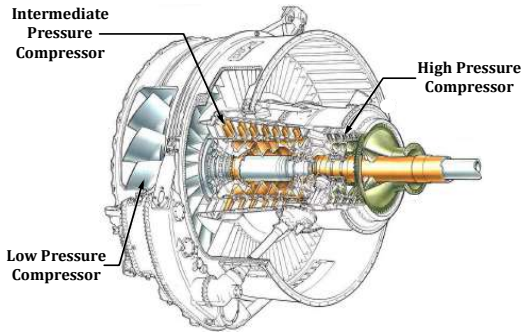


Figure 2.2: Triple spool compressor [4]

## 2.4 The Heat Exchanger

The heat exchanger takes in highly compressed air which fuel is added to and ignited spontaneously since the incoming air temperature is greater than the fuel's thermal ignition temperature. Cool air is channelled on the exterior of the heat exchanger to control the temperature across the walls. Figure 2.3 illustrates the fluid flow through a standard heat exchanger.

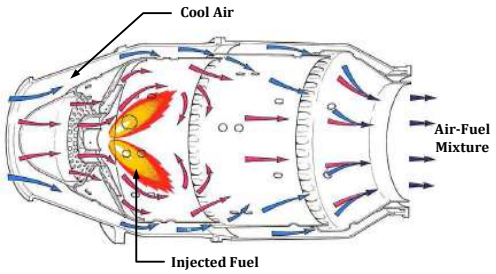


Figure 2.3: Heat exchanger [3].

## 2.5 The Turbine

The air-fuel mixture from the heat exchanger now passes through the turbine and rotates the turbine blades thereby doing work to drive the compressor. The turbine is connected to the compressor via a driveshaft which has a reduction gearbox which to allow more torque to be transferred to the compressor which allows the compressor to achieve greater pressure ratios. This also stops the engine from stalling as the torque allows the compressor to overcome the induced pressures of the exit air of the compressor with the rotation of the turbine assembly. Figure 2.4 illustrates a turbine assembly.

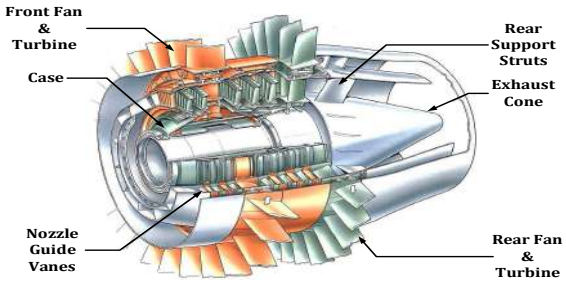


Figure 2.4: Typical Turbine assembly [3].

# Chapter 3

# Methodology / Problem Setup

## 3.1 Apparatus

A complete test rig was used, the Minilab™ Gas Turbine Power System which enclosed the SR-30 Jet engine [13] with the following components:

- Fuel atomization nozzle (with silencer)
- Centrifugal compressor
- Fuel controller
- Annular combustor
- Axial flow turbine
- Thrust nozzle

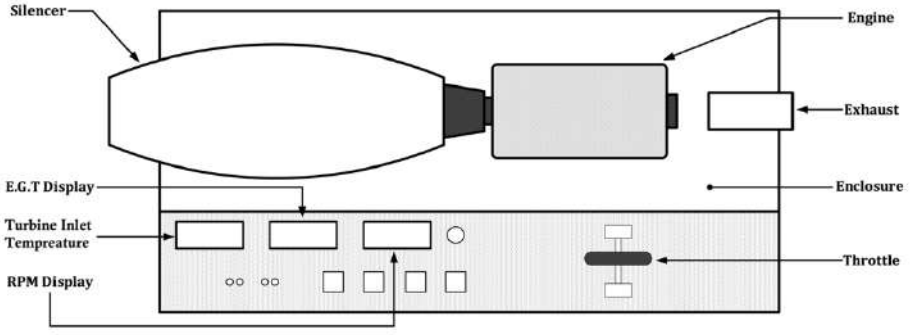


Figure 3.1: Basic layout of the Minilab$^{TM}$ Gas Turbine Power System

This control station displayed in Figure 3.1 allows the operator to control the fuel sent to the engine by adjusting the throttle which will change the speed of the engine.

The speed can be monitored with the RPM display located on the control board, along with the turbine inlet temperature and the exhaust gas temperature on separate dials. Other readings like oil pressure and air-start pressure are also displayed to the operator.

There are sensors attached to each of the previously listed components which are listed with the respective uncertainties:

Table 3.1: Instruments used to measure varies parameters

| **Quantity measured** | **Device used** |
|---|---|
| Pressure at varies stages | Setra Model 256 ($\pm$ 256 PSIG) |
| Thrust force | TTL generator ($\pm$0.5rpm) |
| Fuel flow | Setra Model 209 ($\pm$100 Gal/hr) |
| Temperature at varies stages | K-type Thermocouple |

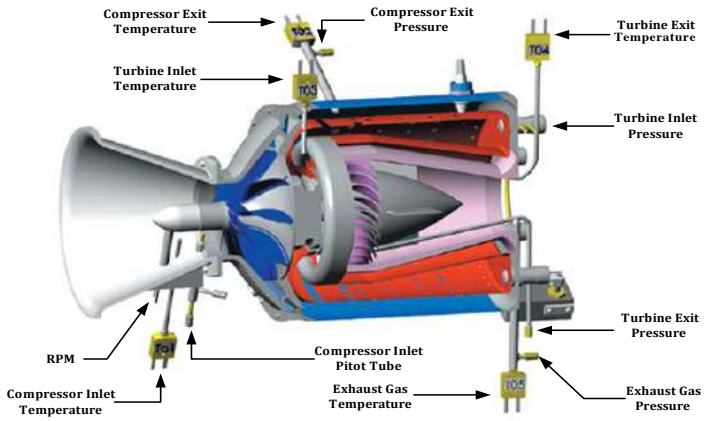


Figure 3.2: SR-30 Jet engine with all recording sensors

## 3.2 Methodology

### 3.2.1 Engine set-up procedure

- The entrance to the laboratory is closed and an extractor fan is switched on which relieves harmful emissions from the enclosed room to the external atmosphere.
- The data acquisition system is enabled and set up to record the required parameters of the engine at a given time interval.

- Power is supplied to the test rig and the engine ignition is switched on so start up can then proceed using a jet of pressurised air.
- Once the engine is at approximately 10 000 rpm, fuel can now be injected and ignited.
- Once the engine speed is approximately 40 000 rpm, switch off the ignition and air as the engine can now sustain itself.

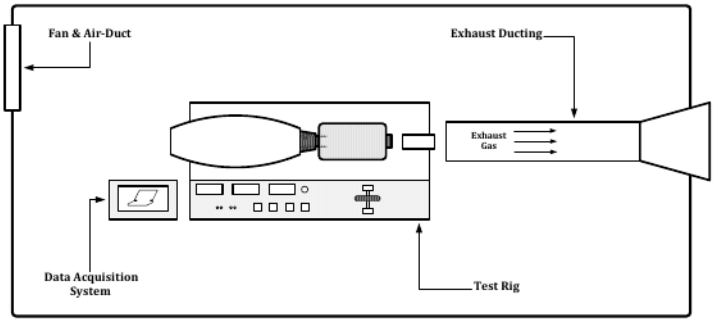


Figure 3.3: Schematic of laboratory layout

### 3.2.2 Operational Procedure

- Once the engine is running, increase the engine speed in increments of 5000 rpm from a minimum of 60 000 rpm to a maximum of 85 000 rpm.
- Allow the engine to reach an equilibrium at each selected speed by leaving the engine idle for approximately 90 seconds for the data acquisition system to record appropriate readings.
- Adjust the engine speed using the throttle to increase speed during a “hot run” and decrease the speed for a “cold run”.
- During each stage of varying engine speeds, the exhaust gas temperature and turbine inlet temperature should be recorded.
- Once the maximum testing speed is achieved, a reduction is speed of equal increments should be conducted and recorded.
- All operating parameters should be recorded by the data acquisition system in addition to the ambient air temperature and pressure.

- Once testing is complete, the engine should be brought back to its idle speed and left to run at this speed for several minutes. This allows the engine to cool down, after which the fuel supply to the engine can be cut. The engine will then spool down until it stops.

## 3.3 Precautions

### 3.3.1 Safety Precautions

- Ear protection is required at all times for everyone present during operation of the gas turbine since the noise produced by the engine and/or extractor fan can cause permanent hearing loss or ear damage.
- The exterior of the exhaust should not be touched throughout the experiment as the operating temperatures are in the region of 600℃.

### 3.3.2 Operating Precautions

- Check fuel and oil pressure is sufficient before starting.
- Turn compressor manually to ensure that it can rotate freely.
- A red-light indicator on the test rig will indicate if the oil pumps are working, however once the engine is running the light should switch off, if light remains on the engine should be switched off as there is a problem with the pumps.
- Ensure the air flowing into the system is undisturbed and uninterrupted.
- Operate the throttle cautiously, to avoid fluctuations in engine speed.
- At each stage of testing the engine should be allowed to reach a steady state. This ensures that the data is representative of the engines performance for that speed.
- Ensure compressor is rotating before starting up.
- Do not allow any foreign material to get sucked in by the compressor.

- Specific temperatures and pressures for different components should never exceed those of which that are listed in Table 3.2:

Table 3.2: Maximum allowable readings

| | |
|---|---|
| Turbine inlet temperature | 900℃ |
| Exhaust gas temperature | 600℃ |
| Oil pressure | 10 – 30 PSI |
| Fuel pressure | 150 – 200 PSI |
| Air pressure | 100 – 150 PSI |

# Chapter 4

# Results and Analysis

## 4.1 Observations

During the initial stages (i.e at low RPM's), flames from the exit nozzle were observed. Once the engine ran up to the higher RPM's, it displayed no distinctive characteristics and continued to operate predictably, producing more noise as the engine speed increased.

The sensors on the test rig measured the operating parameters such as pressures and temperatures at varies points in the cycle, these specific parameters were measured at regular time intervals. Laboratory conditions and various properties were measure which are noted in Table 4.1:

| **Property** | **Value** |
|---|---|
| $\mathrm{P_{atm}}$ | 83640 Pa |
| Density of kerosene | 797 $\mathrm{kg/m^3}$ |
| Density of air | 1.23 $\mathrm{kg/m^3}$ |
| Lower calorific value of kerosene | 43 000 kJ/kg |
| Inlet diameter of compressor | 2.78" |
| Ambient temperature | 17℃ |

## 4.2 Data Processing

From the raw data measured, Figure 4.1 to 4.3 were plotted. All the horizontal lines in these figures represent steady state values. All these values were taken into account by averaging each horizontal line resulting in steady state values for each of the desired RPM's for conducting this experiment.

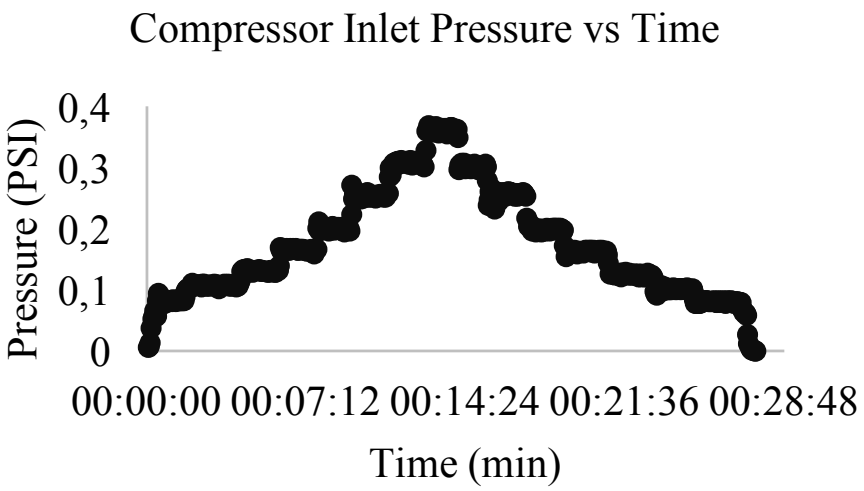


Figure 4.1: Raw data for Compressor Pressure

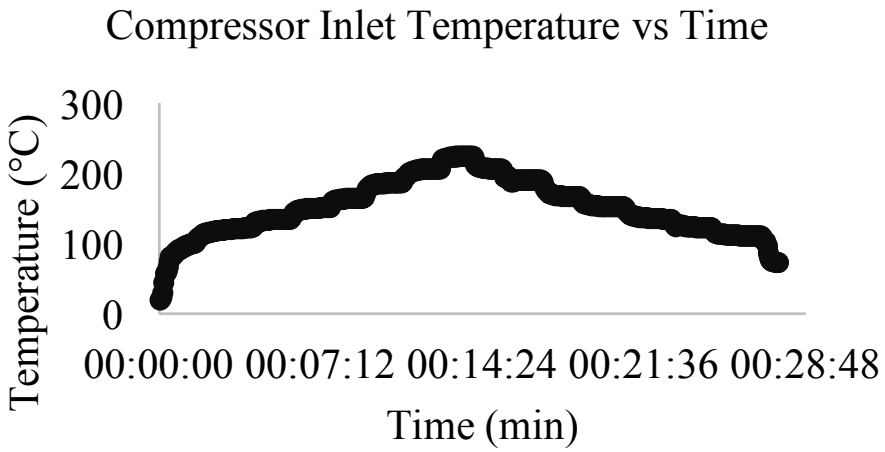


Figure 4.2: Raw data for Compressor temperature

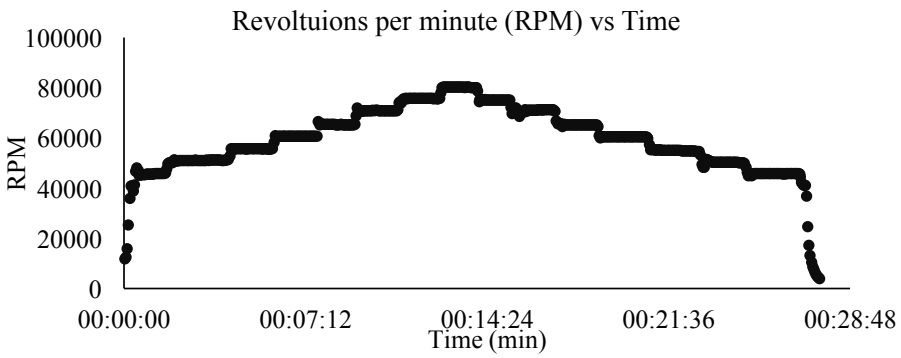


Figure 4.3: Raw Data of RPM vs Time

A complete table with all steady state values for each parameter measured by the data acquisition system can be found in Appendix A.

### 4.2.1 Assumptions

All calculations performed on raw data used an ideal Brayton cycle analysis using an air standard and cold-air standard approach. Specific values listed in Table 4.1 were assumed to be constant, these values were fixed as the temperature variation at particular states was negligible.

Table 4.1: Constant values

| **Constant** | **Value** |
|---|---|
| Specific heat ratio (k) | 1.4 |
| $C_p$ across the turbine | 1.1 kJ/kg |
| $C_p$ across the compressor | 1.0245 kJ/kg |

Other assumptions also considered:

- Each component was modelled as a control volume at steady state with no losses from the system
- When performing an energy balance, the effects of kinetic and potential energy was ignored.

### 4.2.2 Sample Calculations and Uncertainty

A simple calculation was performed on the maximum RPM value which can be found in Appendix B. The uncertainties for key parameters are calculated below:

**Uncertainty for the isentropic compressor exit temperature:**

$$\Delta T_{2s} = \sqrt{\left(\frac{\delta T_{2s}}{\delta T_1}\Delta T_1\right)^2 + \left(\frac{\delta T_{2s}}{\delta p_2}\Delta p_2\right)^2 + \left(\frac{\delta T_{2s}}{\delta p_1}\Delta p_1\right)^2}$$

$$= \sqrt{\left(\left(\frac{p_2}{p_1}\right)^{\frac{k-1}{k}}\Delta T_1\right)^2 + \left(T_1\left(\frac{k-1}{k}\right)\frac{p_2^{-\frac{1}{k}}}{p_1^{\frac{k-1}{k}}}\Delta p_2\right)^2 + \left(-T_1\left(\frac{k-1}{k}\right)\frac{p_2^{\frac{k-1}{k}}}{p_1^{\frac{2k-1}{k}}}\Delta p_1\right)^2}$$

$$= 4.663 \times 10^{-5}\ K$$

**Uncertainty for the isentropic turbine exit temperature:**

$$\Delta T_{4s} = \sqrt{\left(\frac{\delta T_{4s}}{\delta T_3}\Delta T_3\right)^2 + \left(\frac{\delta T_{4s}}{\delta p_4}\Delta p_4\right)^2\left(\frac{\delta T_{4s}}{\delta p_3}\Delta p_3\right)^2}$$

$$= 3.659 \times 10^{-5}\ K$$

**Uncertainty for the compressor efficiency:**

$$\Delta \eta_c = \sqrt{\left(\frac{\delta \eta_c}{\delta T_1}\Delta T_1\right)^2 + \left(\frac{\delta \eta_c}{\delta T_{2s}}\Delta T_{2s}\right)^2 + \left(\frac{\delta \eta_c}{\delta T_2}\Delta T_2\right)^2}$$

$$= 3.868 \times 10^{-4}\%$$

**Uncertainty for the turbine efficiency:**

$$\Delta \eta_T = \sqrt{\left(\frac{\delta \eta_T}{\delta T_3}\Delta T_3\right)^2 + \left(\frac{\delta \eta_T}{\delta T_{4s}}\Delta T_{4s}\right)^2 + \left(\frac{\delta \eta_T}{\delta T_4}\Delta T_4\right)^2}$$

$$= 4.283 \times 10^{-4}\%$$

**Uncertainty for the Carnot cycle efficiency:**

$$\Delta \eta_b = \sqrt{\left(\frac{\delta \eta_b}{\delta T_1}\Delta T_1\right)^2 + \left(\frac{\delta \eta_b}{\delta T_2}\Delta T_2\right)^2}$$

$$= 1.802 \times 10^{-4}\%$$

### 4.2.3 Uncertainty for the SFC value:

$$\Delta SFC = \sqrt{\left(\frac{\partial SFC}{\partial \dot{m}}\Delta\dot{m}\right)^2 + \left(\frac{\partial SFC}{\partial Thrust}\Delta Thrust\right)^2}$$

$$= 1.886 \times 10^{-11}\ kg.kg^{-1}.s^{-1}$$

## 4.3 Results

From the data calculated across the various RPM's using cold-air and the air standard analysis, the graphs in figures 17 to 35 were plotted to analysis the performance of the gas turbine SR-30 used in the experiment. Both a hot run and a cold run were analysed and plotted to effectively determine trends between different parameters.

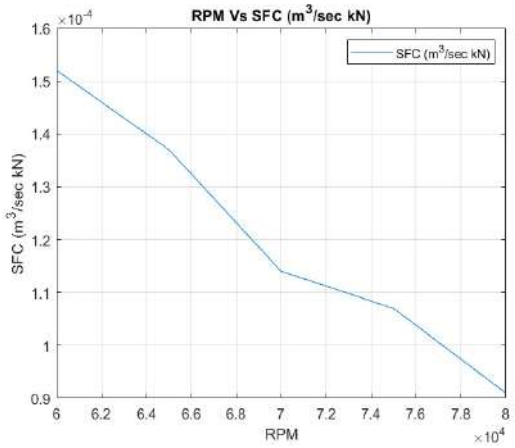


Figure 4.4: Specific Fuel Consumption of engine

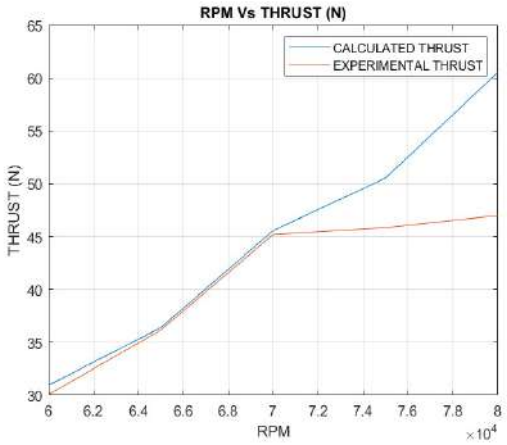


Figure 4.5: Thrust created by engine

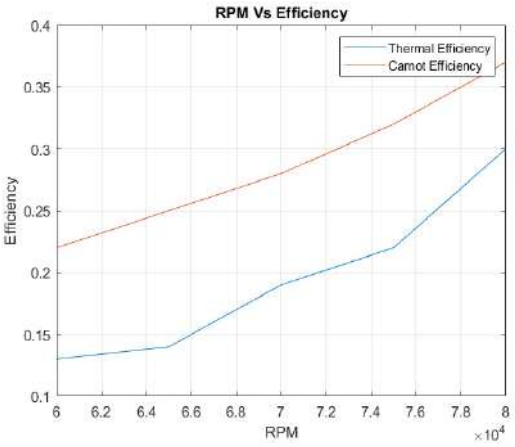


Figure 4.6: Efficiency of Engine compared to the Carnot Efficiency

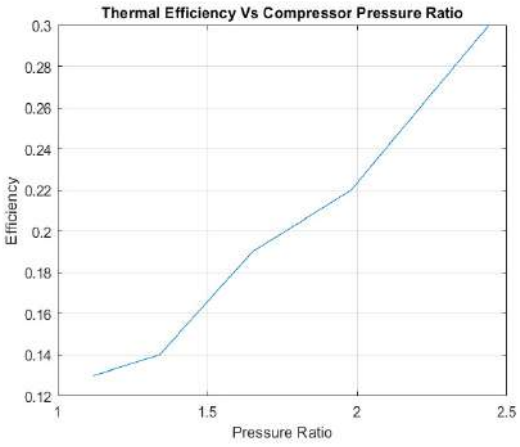


Figure 4.7: Engine Efficiency compared to Pressure ratio

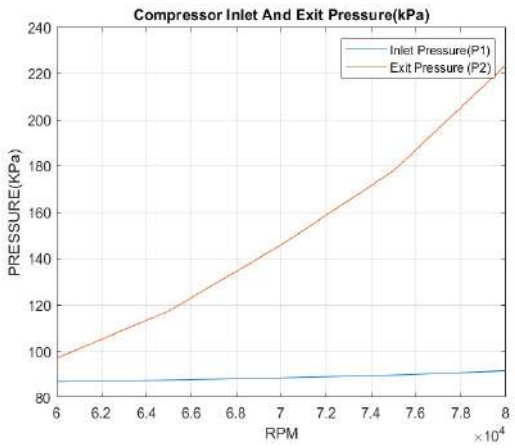


Figure 4.8: Compressure Pressure

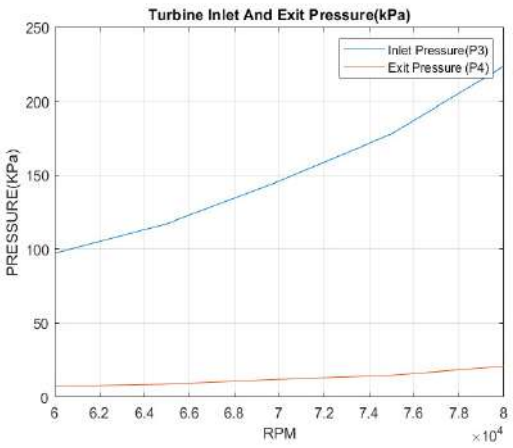


Figure 4.9: Turbine Pressure

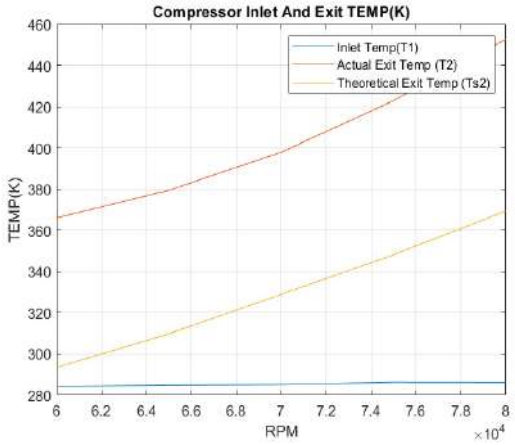


Figure 4.10: Compressor Temperature

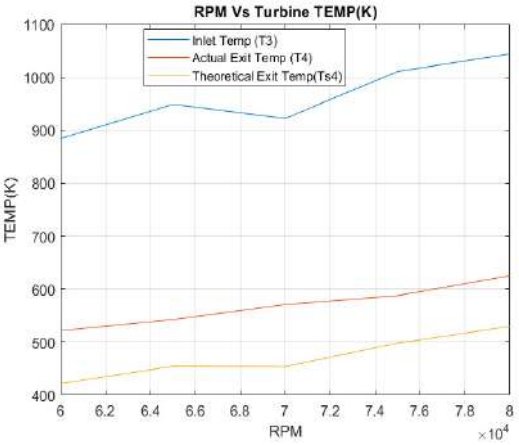


Figure 4.11: Turbine Temperature

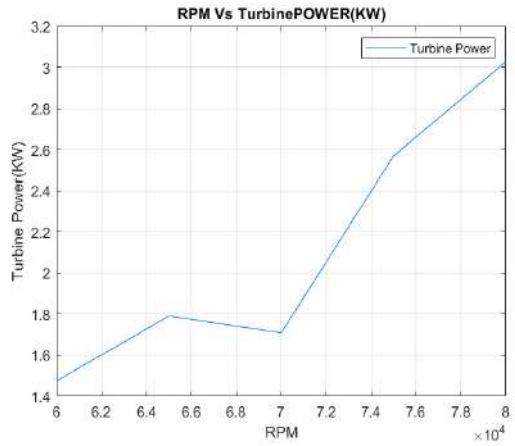


Figure 4.12: Turbine Power

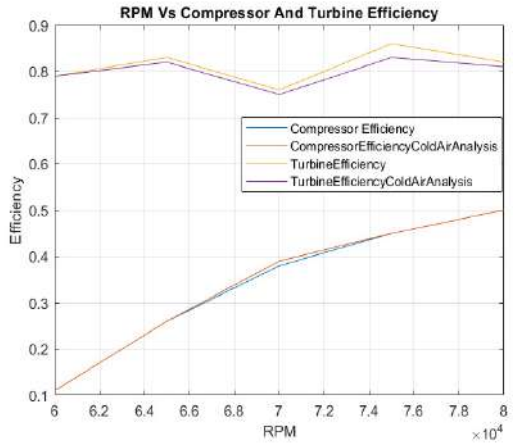


Figure 4.13: Different analysis for Turbine and Compressor Efficiencies

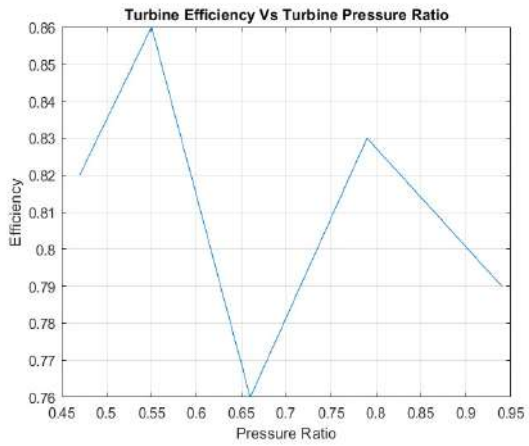


Figure 4.14: Turbine efficiency compared to Pressure Ratio

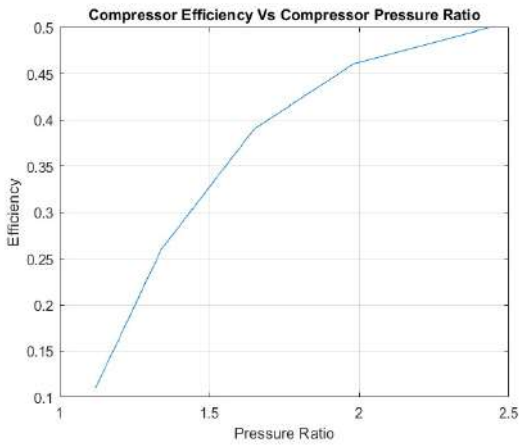


Figure 4.15: Compressor Efficiency compared to Pressure Ratio

## 4.4 Risk Assessment

| Risk type | Risk description | Severity | Likelihood | Risk score | Action Type | Action |
|---|---|---|---|---|---|---|
| Ergonomic | Hearing damage due to noisy environment | Major | Likely | 8 | PPE | Use ear protection at all times during the experiment |
| Mechanical | Turbine operating at high speeds | Major | Possible | 7 | PPE | Stand clear of turbine during operation and ensure all items in the room are securely placed so they do not get sucked in by the compressor. |
| Mechanical | Many wires/cables that someone can trip on | Moderate | Possible | 4 | Procedure | Highlight areas with large amounts of cables or use alternate routes to move around |
| Chemical | Exhaust gases contain CO and CO2 | Major | Certain | 6 | Procedure | Ensure extractor fan is switched on |
| Mechanical | Flammable substances | Major | Possible | 7 | Procedure PPE | Ensure nothing flammable is kept within the room |

# Chapter 5

# Discussion

The single stage, centrifugal compressor from Figure 4.8, the exit pressure of the compressor increased with an increase in RPM from a minimum of 96.90kPa to a maximum of 223.42kPa. At these higher RPM's the mass flow rate of air increases as seen in Table C.3 increasing from an initial 0.0047kg/s to 0.0055kg/s. This indicates that the more air drawn in by the compressor results in a higher exit pressure and higher RPM's. The same trends displayed by the compressor pressure can be confirmed as the compressor temperature relations are analogous to each other.

The compressor efficiency with respect to RPM is shown in Figure 4.13, which indicates that the efficiency of the compressor increases with a higher RPM. The compressor efficiency at the initial 60326 RPM was 11% using the cold-air analysis and 11% with the air standard analysis. The efficiency then increased to a maximum of 50% using both the cold air- and air standard respectively at an engine speed of 80982 RPM, which inherently is the maximum RPM achieved. However, the compressor efficiency reduces again during the cold run to 36.38% and 36.48% using cold-air and air standard analysis respectively. This implies that the compressor is the least efficient at start-up and reaches a maximum efficiency at the maximum engine speed. However, the efficiency at lower RPM's is better when the engine speed is being slowed down (cold run) which could be attributed to conservation of momentum of the engine and the engine consuming more volumetric air flow per unit RPM. Also in Figure 4.13, the analysis for cold-air and air standard both provide results within 1% of each other with the exception of the initial RPM where the air standard analysis provides a difference of 5% higher than the cold-air analysis. In general, the compressor will always be more efficient at higher engine speeds and should lie between 40% to 51% in these

conditions.

The turbine which produces the power for the compressor and the thrust for the system. The minimum and maximum inlet pressures are 97.17kPa and 223.64kPa respectively, which is shown in Figure 4.9 shows the maximum inlet pressure occurs at the maximum of 82982 RPM. This proves the thermodynamic theory that pressure is constant through a heat exchanger which only increases the temperature of the working fluid, as the exit pressure from the compressor is seen as the turbine inlet pressure. This results in the turbine displaying the same treads as the compressor with respect to the pressure verses RPM as seen in Figure 4.9. The turbine exit pressure is higher than the atmospheric pressure at all RPM's, which implies that the total internal energy from the working fluid after combustion does not transfer to the turbine work [8]. The working fluid is expected to expand from the turbine exit pressure through the nozzle to the atmospheric pressure and thus creating thrust.

When the expansion of the working fluid through the turbine occurs, it is anticipated that the internal energy of the working fluid transfers energy to the turbine, this would result in the turbine exit temperature being less than the inlet temperatures to the turbine, by looking at Figure 4.11, this is not the case. When looking at the turbine efficiencies in Figure 4.13, there is a basic trend that the efficiency increases with RPM, although there is not a definitive trend with the cold-air and air standard analysis like the compressor. There are also negative efficiencies in the lower RPM values, this indicates that the turbine transfers energy to the working fluid, during the expansion process. This is impossible as it represents a perpetual device [14]. Figure 4.12 also displays no coherent results as the cold-air and air standard analysis do not correspond for the turbine power verses RPM as most values are scattered. Possible justification for this coherent error, is that the temperature sensor that measure the turbine exit temperature is defective as combustion deposits settle on the sensor and alter the readings taken. Another reason that could attribute to this problem is the fuel delivery system, there is incomplete combustion in the air-fuel mixture which travels through the turbine. Therefore, no conclusion can be drawn about the turbines actual performance as the fundamental raw data values measured are incorrect. Therefore, turbine efficiencies and power analysis could not be completed effectively.

From Figure 4.5, the expected thrust and actual thrust produced is moderately

linear with an increase in RPM. It also can be deduced that more thrust is produced when the engine is warm is greater than when the engine is in the initial stages. During the initial speed of 60326 RPM the measured thrust was 30N and the calculated thrust was 31N. This shows that even at a lower RPM the engine produced more thrust when the engine is warm and decreasing in RPM. It is also seen in Figure 4.5 that the measured thrust is always lower than the calculated thrust from equation 1.7. This is because equation 1.7 does not account of losses and irreversibilities in the system, therefore the equation will always overestimate the actual thrust that an engine can develop.

The specific fuel consumption (SFC), is the amount of fuel used per unit time per unit thrust. This is effectively the fuel efficiency of the engine. As seen in Figure 4.4, the SFC decreases as the RPM increases, this means that the engine is consuming less fuel as the RPM is increased, making the engine more efficient at higher RPM's. Even though at higher RPM's the fuel flow rate is higher, the amount of thrust it produces with increased engine speed surpasses the rate at which it consumes fuel. It can also be seen that less fuel is consumed when the engine is slowing down, as the SFC at the initial RPM of 60326 is 0.000152 $\mathrm{m}^3/\mathrm{s}$ kN compared to 0.0009029$\mathrm{m}^3/\mathrm{s}$ kN when the engine is returning to an RPM of 60326. Which means that accelerating the engine creates a greater fuel strain with direct proportionality. The minimum SFC value is 0.000091 $\mathrm{m}^3/\mathrm{s}$ kN which occurred at the maximum RPM value of 82982, this minimum value would indicate the area where maximum efficiency would occur.

The propulsion efficiency is calculated using equation 1.9, however in this equation the numerator is Va which is the velocity of the entire aircraft through the air. In this experiment, the test rig was fixed to a stationary position on the laboratory. Va then is zero and the entire propulsion efficiency term is also zero. This does support the definition of propulsion efficiency as it represents how well energy is converted into useful propulsion [9]. Since the test rig is stationary, there can be no raw data to measure actual propulsion to compare the propulsive energy capable of the system in order to generate an efficiency. For this reason, only the thermal efficiency will be considered as a reliable gauge for performance for this gas turbine.

The thermal efficiency of the cycle is calculated specifically for a gas turbine using equation 1.8 as the general thermodynamic equation for thermal efficiency would

not be suitable as it uses data from the turbine which has been proved inconclusive. Equation 1.8 uses the fundamental principle of gas turbines by measuring the air-fuel ratio used with the kinetic energy produced compared to how much energy is stored in the fuel by its lower calorific value. This thermal efficiency displays a linear trend in Figure 4.6 against RPM, which means that the maximum efficiency will occur at the maximum RPM. This result is supportive of the conclusion reached when analysing Figure 4.4 with the SFC. In Figure 4.6, the thermal efficiency calculated for the gas turbine is always less than the anticipated Carnot efficiency and this is expected as there are many losses and irreversibilities within the system, so it would always be impossible to achieve the Carnot efficiency. The closest to the Carnot efficiency occurs at the maximum RPM where the Carnot efficiency is 37% while the calculated thermal efficiency is 30%.

From equation 1.5 for a cold-air standard ideal Brayton cycle, the Carnot thermal efficiency only depends on the pressure ratio of compressor, which is dependent on the RPM the engine is operating at. By considering the theoretical thermodynamic plot in Figure 1.6 with anticipated thermal efficiency against the compressor pressure ratio, the cycle becomes asymptotic as the efficiency tends to 60% and therefore an increase in the pressure ratio across the compressor would not increase the thermal efficiency. However, by looking at Figure 1.5 which compares the work and efficiencies on a Ts plot of two different gas turbine cycles, it can be seen that when increasing the pressure ratio to increase the efficiency of the cycle, the area enclosed of the Ts plot is reduced. This area represents the net work of the system. Therefore, a gas turbine with high a thermal efficiency would produce very little work or require a large mass flow rate to achieve the same work. For this reason, the ideal operating

Efficiency for a gas turbine should be between 20% to 50%. By looking at Figure 4.7 and 4.15, the thermal efficiency and compressor efficiency increases with an increase in compressor pressure ratio although, the pressure ratio and efficiency is capped as the net work produced had to have been a finite number at each stage.

With the various assumptions, idealisations and appropriate modelling it can be determined that the method of analysation used is fairly accurate when modelling a gas turbine. Both cold-air and air standard provide reasonable results with marginal uncertainties. The issues with the turbine lead to inconclusive results regarding the

turbine, but the rest of the components and the thermal efficacy could be accurately modelled and when compared to theory, similar findings was presented.

# Chapter 6

# Conclusion

- The efficiency of the compressor which was around 40%, is dependent on the pressure ratio across the compressor, which is dependent on the speed of the engine and is higher when the engine is warm.
- No clear conclusion could be reached with regard to the efficiency of the turbine, as there were errors with the fuel delivery.
- The calculated thermal efficiency of the cycle was always less than the Carnot efficiency, the Carnot efficiency gave a comparison as to where the thermal efficiency was closest to a maximum which was at the higher engine speeds where there was only a 5% difference.
- The measured thrust was always less than the calculated thrust, the measured thrust was more than half the anticipated calculated thrust values. The decrease was as a result of energy losses and irreversibilities.
- The thermal efficiency of the cycle is dependent only on the pressure ratio of the compressor. The engine operated in a viable region of 18% to 41%, which predicted by thermodynamic theory is an acceptable range for efficiency and net work.
- The SFC of the engine decreases as the speed of the engine increases, indicating that the thrust generated surpasses the fuel consumption rate with respect to an increase in engine speed.
- There was a significant increase in efficiency and decrease in SFC when decreasing engine speed as to accelerating to a higher speed with an increase in 9% in efficiency and - 0.0000135$\mathrm{m}^3/\mathrm{s\ kN}$ in SFC.

# Appendices

# Appendix A

Table A.1: Averaged Data Set 1

| RPM | Revolutions rad/s | Time Value (min) | Fuel Flow (Kg/sec) | Thrust (N) |
|---|---|---|---|---|
| 60326.04 | 6345.817 | 0.004757 | 0.0038 | 30.08 |
| 64954.46 | 6829.969 | 0.005938 | 0.0040 | 36.17 |
| 70491.79 | 7414.431 | 0.007049 | 0.0045 | 45.21 |
| 75963.39 | 7924.633 | 0.008252 | 0.0055 | 45.86 |
| 82982.44 | 8390.300 | 0.009282 | 0.0066 | 46.99 |

Table A.2: Averaged Data Set 2

| RPM | Comp Inlet P1 (kPa) | Comp Exit P2 (kPa) | Turb Inlet P3 (kPa) | Turb Exit P4 (kPa) | Noss Exit P5 (kPa) |
|---|---|---|---|---|---|
| 60326 | 3.17 | 96.90 | 97.17 | 7.35 | 6.88254 |
| 64954 | 3.83 | 117.33 | 117.30 | 8.92 | 8.30711 |
| 70491 | 4.83 | 145.86 | 145.99 | 12.20 | 11.52781 |
| 75963 | 6.01 | 177.88 | 177.86 | 14.97 | 14.50509 |
| 82982 | 7.80 | 223.42 | 223.64 | 20.80 | 17.49646 |

Table A.3: Averaged Data Set 3

| RPM | Comp Inlet T1 (K) | Comp Exit Temp T2 (K) | Turb Inlet Temp T3 (K) | Turb Exit Temp T4 (K) | EGT T5 (K) |
|---|---|---|---|---|---|
| 60326.04 | 284.30 | 365.98 | 884.08 | 521.38 | 709.26 |
| 64954.46 | 284.88 | 379.45 | 948.96 | 542.48 | 739.81 |
| 70491.79 | 285.14 | 397.52 | 922.30 | 571.23 | 737.13 |
| 75963.39 | 286.24 | 422.90 | 1010.77 | 587.82 | 757.87 |
| 82982.44 | 286.15 | 452.17 | 1043.71 | 625.14 | 804.13 |

# Appendix B

| Units | Value |
|---|---|
| PSI to Pa | x6894.76 |
| Gal/hr to $m^3/s$ | x$6.31 \times 10^{-5}$ |
| Lbs to kg | x0.453592 |
| Lbs to N | x4.44822 |
| RPM to rad/s | x0.10472 |
| ℃ to Kelvin | +273.15 |
| L/hr to kg/sec | x0.00028 |

## Cold Air Analysis

### Isentropic Compressor exit temperature

$$T_{2s} = T_1 \left( \frac{p_2}{p_1} \right)^{\frac{k-1}{k}}$$
$$T_{2s} = 369.357 \text{ K}$$

### Isentropic Turbine exit temperature

$$T_{4s} = T_3 \left( \frac{p_4}{p_3} \right)^{\frac{k-1}{k}}$$
$$T_{4s} = 529.491 \text{ K}$$

### Carnot Cycle Efficiency

$$\eta_b = \left(1 - \frac{T_1}{T_2}\right)$$
$$\eta_b = 0.367$$

## Air Standard Analysis

$$\frac{P_1}{P_2} = \frac{p_{r1}}{p_{r2}}$$

### Compressor

$$\eta_c = \frac{h_{2s} - h_1}{h_2 - h_1} :$$
$$[\eta_c = 0.50$$

From Table A-17 @Cengel Thermodynamics Ed 9

$@T_{2s} = 369.357$ K , $h_{2s} = 369.51$ KJ/Kg , @$T_1 = 286.15$ K $h_1 = 286.14$ KJ/Kg , @$T_2 = 452.17$ K , $h_2 = 452.80$ KJ/Kg

### Turbine

$$\eta_t = \frac{h_3 - h_4}{h_3 - h_{4s}}$$
$$\eta_t = 0.821$$

From Table A-17 @Cengel Thermodynamics Ed 9

@$T_{4s} = 529.491$ K , $h_{4s} = 533.40$ KJ/Kg , @$T_3 = 1043.71$ K , $h_3 = 1091.85$ KJ/Kg , @$T_4 = 625.14$ K , $h_4 = 633.14$ KJ/Kg

### Exit Velocity

$$V_5 = \sqrt{\frac{2 \cdot P_5}{\rho_{air}}}$$
$$V_5 = 182.50 \frac{m}{s}$$

## Kinetic Energy

$$ke_5 = \frac{V_5^2}{2}$$
$$ke_5 = 16653.06\ \frac{kj}{kg}$$

## SFC

$$SFC = \frac{\dot{m}}{Thrust}$$
$$SFC = 0.0.000109\ \mathrm{m}^3/\mathrm{sec\ kN}$$

## Thrust

$$Thrust = \dot{m} \times \textit{Exit Velocity}$$
$$Thrust = 61\ N$$

## Thermal Efficiency

$$\eta_b = \frac{\dot{m}_{air} ke_5}{\dot{m}_{fuel}(\text{Calorific value})} = 0.30$$

## Propulsion Efficiency

$$\eta_{propulsive} = \frac{V_a}{V_5 + V_a} = \frac{0}{182.50 + 0} = 0$$

# Appendix C

# Important Values from Processed Data

Table C.1: Processed Data 1

| RPM | P2/P1 | Comp Efficienc (Cold air analysis) | Comp Efficiency (Air standard analysis) | P4/P3 | Turbine Efficiency (Cold Air analysis) | Turbine Efficienc (Air Standard-analysis) | Carnot Cycle Efficiency (1 - T1/T2) |
|---|---|---|---|---|---|---|---|
| 60326 | 1.12 | 0.11 | 0.11 | 0.94 | 0.79 | 0.79 | 0.22 |
| 64954 | 1.34 | 0.26 | 0.26 | 0.79 | 0.82 | 0.83 | 0.25 |
| 70492 | 1.65 | 0.39 | 0.39 | 0.66 | 0.75 | 0.76 | 0.28 |
| 75963 | 1.98 | 0.45 | 0.46 | 0.55 | 0.83 | 0.86 | 0.32 |
| 82982 | 2.44 | 0.50 | 0.50 | 0.47 | 0.81 | 0.82 | 0.37 |

Table C.2: Processed Data 2

| RPM | V5 m/s | Kinetic Energy (ke5) J/kg |
|---|---|---|
| 60326 | 109.25 | 5967.35 |
| 64954 | 120.01 | 7200.82 |
| 70492 | 140.61 | 9885.71 |
| 75963 | 155.35 | 12066.12 |
| 82982 | 182.50 | 16653.06 |

Table C.3: Processed Data 3

| **RPM** | **Thrust (actual) N** | **Thrust (Calculated) N** | **Fuel Flow L/Hr** | **SFC ($m^3$/s kN)** | **$\dot{m}$ air kg/s** | **$\dot{m}$ fuel kg/s** | **$\dot{m}$ Total kg/s** | **Thermal efficiency** |
|---|---|---|---|---|---|---|---|---|
| 60326 | 30 | 31 | 17.00 | 0.000152 | 0.431 | 0.0047 | 0.435 | 0.13 |
| 64954 | 36 | 36 | 18.20 | 0.000137 | 0.431 | 0.0050 | 0.436 | 0.14 |
| 70492 | 45 | 46 | 19.45 | 0.000114 | 0.431 | 0.0052 | 0.437 | 0.19 |
| 75963 | 46 | 51 | 19.52 | 0.000107 | 0.431 | 0.0054 | 0.439 | 0.22 |
| 82982 | 47 | 61 | 19.90 | 0.000091 | 0.431 | 0.0055 | 0.440 | 0.30 |

# Bibliography


[1] J. Moran, M and N. Shapiro, H, *Fundamentals of Engineering Thermodynamics*. 7th ed. (SI Version), John Wiley & Sons, West Sussex, England, 2012.

[2] Y. Cengel and M. Boles, *Thermodynamics*. 8th ed. New York: McGraw-Hill Education, 2015.

[3] M. J. Zucrow, *Aircraft and missile propulsion*, vol. 1. 1st ed. USA: John Whiley & Sons, 1958.

[4] G. G. Smith and F. Sheffield, *Gas turbines and jet propulsion*. 6th ed. London: Whitefriars Press Ltd, 1955.

[5] D. Shepherd, *Aerospace Propulsion*. 1st ed. New York: American Elsevier Publishing Company, 1972.

[6] J. Kerrebrock, *Aircraft engines and gas turbines*. 1st ed. USA: The Alpine Press, 1977.

[7] O. E. Lancaster, *Jet Propulsion Engines*, vol. 2247. 3rd ed. New Jersey: Princeton University Press, 1959.

[8] N. Cumpsty, *Jet Propulsion*. 3rd ed., Cambridge University Press, Cambridge, United Kingdom, 2005.

[9] P. G. Hill and C. R. Peterson, *Mechanics and Thermodynamics of Propulsion*. 3rd ed. USA: Addison Wesley Publishing Company, 1992.

[10] W. Smith, Chester, *Aircraft Gas Turbines*. 1st ed. London: John Wiley & Sons, 1956.

[11] I. E. Treager, *Aircraft Gas Turbine Engine Technology*. 2nd ed. USA: McGraw-Hill, 1979.

[12] R. Peterson, Carl, *Mechanics & Thermodynamics of Propulsion*. 2nd ed. USA: Addison Wesley Publishing Company Inc, 1992.

[13] A. Skrotzki G and A. Vopat, W, *Steam and Gas Turbines*. McGraw-Hill , New York , 1st Edition, 1950.

[14] R. Royce, *The Jet engine*. 3rd ed. England: Product Support Graphics Ltd, 1973.